Intrinsic Quantum Beats of Atomic Populations and Their Nanoscale Realization Through Resonant Plasmonic Antenna

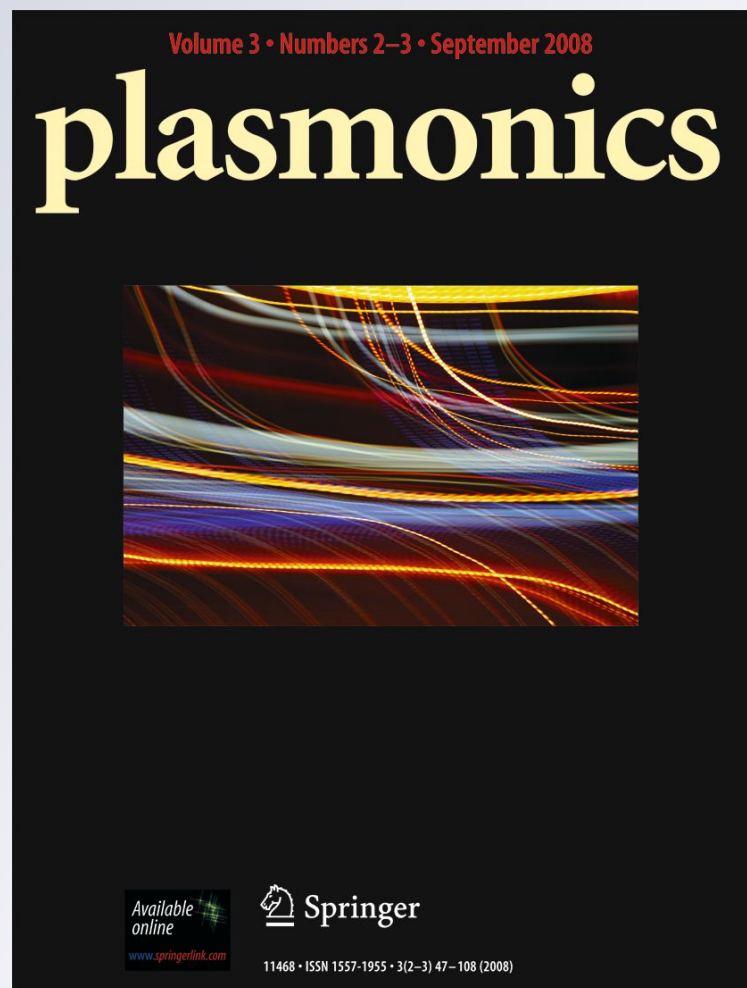## Ying Gu, Luojia Wang, Pan Ren, Junxiang Zhang, Tiancai Zhang, Jing-Ping Xu, Shi-Yao Zhu & Qihuang Gong

Springer

Intrinsic Quantum Beats of Atomic Populations and Their Nanoscale Realization Through Resonant Plasmonic Antenna

**Ying Gu · Luojia Wang · Pan Ren · Junxiang Zhang ·
Tiancai Zhang · Jing-Ping Xu · Shi-Yao Zhu ·
Qihuang Gong**

Abstract In the coherently trapped populations of a four-level atom, we demonstrated the quantum beats with different mechanism, which originate from the interference between transition channels with different dipole moments. The beat frequency is determined by the intrinsic atomic parameters, i.e., the spacing of upper levels and ratio of dipole moments. The resonant plasmonic nanoantenna, as a candidate for the creation of anisotropic vacuum, was proposed to achieve the nanoscale realization of the quantum beats, spontaneous emission cancellation, and Rabi oscillation in two-photon correlations through the enhanced near-field and modified decay rates.

Keywords Quantum beats · Quantum interference ·
Surface plasmon · Anisotropic vacuum ·
Local field distribution

Y. Gu (✉) · L. Wang · P. Ren · Q. Gong
State Key Laboratory for Mesoscopic Physics,
Department of Physics, Peking University,
Beijing 100871, China
e-mail: ygu@pku.edu.cn

Q. Gong
e-mail: qhgong@pku.edu.cn

J. Zhang · T. Zhang
State Key Laboratory of Quantum Optics and Quantum
Optics Devices, Institute of Opto-Electronics,
Shanxi University, Taiyuan 030006, China

J.-P. Xu
Department of Physics, Tongji University,
Shanghai 200092, China

S.-Y. Zhu
Beijing Computational Science Research Center,
Beijing 100084, China

Introduction

Quantum interferences (QIs) in multilevel atomic systems are generally concerned with extrinsic atomic parameters. Spectral line cancellation of spontaneous emission is induced by the coherent trapping of populations of upper closing levels [1, 2]. By adjusting the phase and pulse envelope of the pumping field, a continuous transition from narrowing to elimination in fluorescence spectra is reported [3–5]. QI can also be induced by an anisotropic vacuum [6]. In photonic band gap structures, interference between transition channels leads to the population oscillations of two upper levels [7, 8]. Through light focusing and phase compensation in a left-handed material, QI between two orthogonal dipoles is realized [9]. The anisotropy of the electric modal density coming from the collective oscillations of free electrons in metals enhances the QI effects [10]. In this work, instead of the interferences induced by the extrinsic atomic parameters, we propose the interference with a totally different mechanism, i.e., quantum beats of population oscillations, determined by the intrinsic atomic parameters.

By squeezing light into nanoscale volumes, photonic structures with evanescent fields in nanoregions, especially plasmonic elements [11–16], allow for the nanoscale realization of light matter interactions that are not accessible through traditional techniques. Through modifying the population of excited states and decay rate of quantum emitters near plasmon structure, the emission spectra of fluorescent molecules and semiconductor quantum dots can be controlled [17]. Through the nanoscale coupling between the surface plasmons of a silver nanowire and a single quantum emitter, the directional emission and high-efficiency

generation of single photons can be achieved [12]. Using localized plasmon coupling, selective enhancement of surface-state emission in CdS nanocrystals was proposed [13]. Through the near-field enhancement and decay rate modification in plasmonic structures, nanoscale control of the Mollow triplet of the molecular fluorescence spectrum and antibunching of emission photons is demonstrated [14, 15]. Using the evanescent fields of tapered optical fibers, sharply peaked two-photon absorption in rubidium vapor was observed at low power levels [16]. Here, the nanoscale realization of the proposed quantum phenomenon was demonstrated through a resonant plasmonic nanoantenna.

We first set the trapping condition allowing the populations to coherently stay in the closing upper levels of four-level atom. For this case, we found the transient quantum beats in the population oscillations originating from interference between transition channels with different dipole moments in the isotropic and anisotropic vacuum. Unlike the QIs induced by extrinsic parameters [1–10], beat frequencies are determined by the intrinsic atomic parameters, i.e., the spacing of two upper levels and ratio of the two dipole moments. These parameters can be monitored via changes in Rabi frequency in spontaneous emission spectra and two photon correlations; therefore, the system may have potential applications in the measurement of dipole moments [18]. Next, a resonant plasmonic nanoantenna [19], which can induce an anisotropic vacuum, was used to achieve the nanoscale realization of quantum beats, spontaneous emission cancellation, and Rabi oscillation in two photon correlations through the enhanced near-field and modified decay rates.

Quantum Beats of Atomic Populations in Isotropic Vacuum

Consider the four-level atom with two closing upper states $|a_1\rangle$ and $|a_2\rangle$ and two ground states $|b\rangle$ and $|c\rangle$, which is shown in the inset of Fig. 1. The transitions $|a_1\rangle \leftrightarrow |b\rangle$ and $|a_2\rangle \leftrightarrow |b\rangle$ are coherently driven by a pump field with frequency ν, Rabi frequencies Ω_1 and Ω_2, and the detunings $\Delta_1 = \omega_{a_1} - \nu$ and $\Delta_2 = \omega_{a_2} - \nu$ where $\omega_{a_1} - \omega_{a_2} = \omega_{12}$, respectively. Spontaneous emission from $|a_1\rangle$ and $|a_2\rangle$ to $|c\rangle$ are coupled via the kth isotropic or anisotropic vacuum mode which has frequency ω_k and coupling constants $g_k^{(1,2)}$. If the initial vector state is $|\psi(0)\rangle = \{A_1(0)|a_1\rangle + A_2(0)|a_2\rangle + B(0)|b\rangle\}|0\rangle$, in the dipole, rotating-wave, and Wigner–Weisskopf approximations, the state vector $|\psi(t)\rangle = \{A_1(t)|a_1\rangle + A_2(t)|a_2\rangle + B(t)|b\rangle\}|0\rangle + \sum_k C_k(t) b_k^+|0\rangle|c\rangle$, which obey
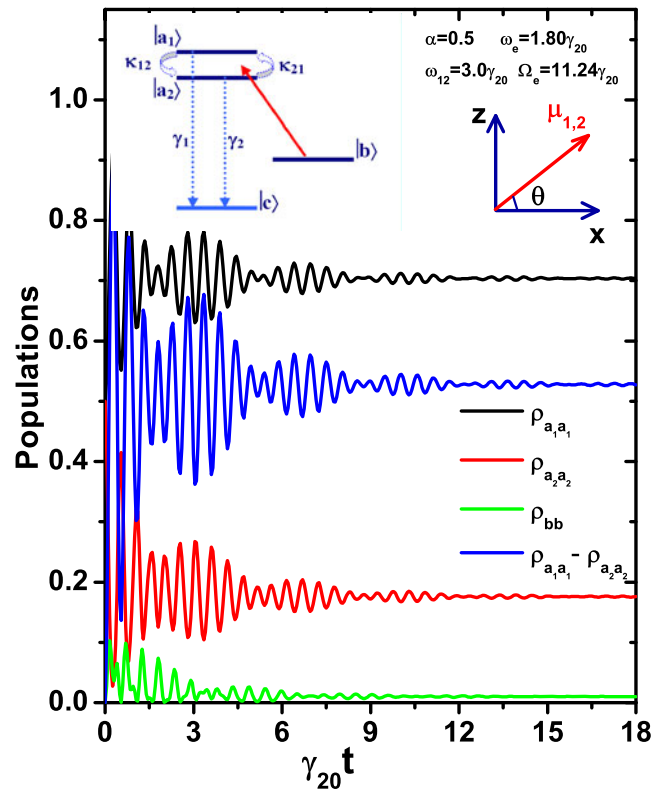

Fig. 1 Quantum beats in the population oscillations in the isotropic vacuum with the parameters $\gamma_{20} = 1.0$ and $\theta = 0.0$. The *insets* are schematics of the four-level system and dipole moments

the Schrodinger equation, can be written as: [1, 2, 10, 20]

$$\frac{d}{dt} A_1(t) = -\frac{\gamma_1}{2} A_1(t) - \frac{\kappa_{12}}{2} A_2(t) e^{i\omega_{12}t} + \Omega_1 e^{i\Delta_1 t} B(t),$$

(1a)

$$\frac{d}{dt} A_2(t) = -\frac{\gamma_2}{2} A_2(t) - \frac{\kappa_{21}}{2} A_1(t) e^{-i\omega_{12}t} + \Omega_2 e^{i\Delta_2 t} B(t),$$

(1b)

$$\frac{d}{dt} B(t) = -\Omega_1^* e^{-i\Delta_1 t} A_1(t) - \Omega_2^* e^{-i\Delta_2 t} A_2(t),$$

(1c)

$$\frac{d}{dt} C_k(t) = -g_k^{(1)} A_1(t) e^{-i(\omega_{a_1 c} - \omega_k)t} - g_k^{(2)} A_2(t) e^{-i(\omega_{a_2 c} - \omega_k)t},$$

(2)

where γ_1 and γ_2 are the decay rates from the upper two levels to lower level and κ_{12} and κ_{21} are the crossing damping terms between $|a_1\rangle$ and $|a_2\rangle$. For the closing states $|a_1\rangle$ and $|a_2\rangle$, we have $\kappa_{12} = \kappa_{21} = \kappa$. In an anisotropic vacuum, if y-axis is quantum axis, the values of $\gamma_{1,2}$ and κ are $\gamma_{1,2} = \gamma_{(1,2)0}(\frac{6\pi c}{\omega_{ac}})[ImG_{xx}\cos^2\theta_{1,2} + ImG_{zz}\sin^2\theta_{1,2}]$ and $\kappa = \sqrt{\gamma_{10}\gamma_{20}}(\frac{6\pi c}{\omega_{ac}})[ImG_{xx}$

$\cos \theta_1 \cos \theta_2 + ImG_{zz} \sin \theta_1 \sin \theta_2]$, respectively [14, 15, 21, 22]. In this case, $\theta_{1,2}$ are the intersection angles between the dipole moments $\vec{\mu}_{1,2}$ and the x-axis; $G_{\beta\beta}$ with $\beta = x, y, z$ is the Green's tensor; and $\gamma_{(1,2)0} = \mu_{(1,2)}^2 \omega_{ac}^3/(3\pi\epsilon_0\hbar c^3)$ are the decay rates in an isotropic vacuum. We will assume that the ratios of the dipole moments between the two upper levels and the levels $|b\rangle$ and $|c\rangle$ are the same. The anisotropic vacuum can be created by the metamaterial, plasmonic structure, and layered waveguide, and the quantum coherences have been widely studied especially for the orthogonal case $\vec{\mu}_1 \cdot \vec{\mu}_2 = 0$ [9, 10, 23].

To ensure that the populations are coherently trapped in the upper levels, Eq. 1 must have a nonzero steady-state solution, i.e., $\lambda = 0$ [1, 2]. This requires that

$$\gamma_1|\Omega_2|^2 + \gamma_2|\Omega_1|^2 - \kappa(\Omega_1\Omega_2^* + \Omega_2\Omega_1^*) = 0, \quad (3a)$$

$$\Delta_1|\Omega_2|^2 + \Delta_2|\Omega_1|^2 = 0. \quad (3b)$$

Therefore, the previous trapping condition in the isotropic vacuum [1, 2] can extend to the anisotropic vacuum. After further consideration, we found that only when $\theta_1 = \theta_2$, i.e., two dipole moments are parallel, the above trapping conditions are fulfilled. If we put atoms near the resonant plasmonic structure, the decay

rates $\gamma_{1,2}$ and κ, as well as the drive Rabi frequencies $\Omega_{1,2}$, can be controlled at the nanoscale [14, 15].

For the trapping condition, the cubic equation, which is similar to Eq. 7 in [1, 2], is quadratic:

$$\lambda^2 - \lambda(\Gamma_1 + \Gamma_2) + \left[\Gamma_1\Gamma_2 + |\Omega_1|^2 + |\Omega_2|^2 - \frac{\kappa^2}{4}\right] = 0, \quad (4)$$

where $\Gamma_{1,2} = \gamma_{1,2}/2 + i\Delta_{1,2}$. Now we let $\theta_1 = \theta_2 = \theta$, $|\vec{\mu}_1|/|\vec{\mu}_2| = \alpha$ and $(\gamma_1 + \gamma_2)/2 = \gamma$ and define the effective spacing $\omega_e = \frac{1-\alpha^2}{1+\alpha^2}\omega_{12}$ and effective Rabi frequency $|\Omega_e|^2 = [\frac{\alpha}{1+\alpha^2}\omega_{12}]^2 + |\Omega_1|^2 + |\Omega_2|^2$. When $(\gamma - i\omega_e)^2 << 4|\Omega_e|^2$, we have $\lambda_{1,2} \doteq \frac{\gamma}{2} - i\frac{\omega_e}{2} \pm i|\Omega_e|$. Substituting $A_1(t) = (e^{-\lambda_1 t}\alpha_1 + e^{-\lambda_2 t}\alpha_2 + \alpha_3)e^{i\Delta_1 t}$, where α_1, α_2, α_3 correspond to the initial state $A_1(0)$, of the population evolution, we obtain:

$$\rho_{a_1 a_1}(t) = \rho_{a_1 a_1}^{(0)}(t) + \rho_{a_1 a_1}^{(1)}(t) + \rho_{a_1 a_1}^{(2)}(t), \quad (5)$$

where the term $\rho_{a_1 a_1}^{(0)}(t) = |\alpha_1|^2 e^{-[\lambda_1+\lambda_1^*]t} + |\alpha_2|^2 e^{-[\lambda_2+\lambda_2^*]t} + |\alpha_3|^2$ is the trapping term and approaches $|\alpha_3|^2$ as t approaches infinity. $\rho_{a_1 a_1}^{(1)}(t) = \alpha_1^*\alpha_3 e^{-\lambda_1^* t} + \alpha_2^*\alpha_3 e^{-\lambda_2^* t} + \alpha_1\alpha_3^* e^{-\lambda_1 t} + \alpha_3^*\alpha_2 e^{-\lambda_2 t}$ is related to the population oscillations and quantum beats. Moreover, the effect of the high-frequency terms $\rho_{a_1 a_1}^{(2)}(t) = \alpha_1\alpha_2^* e^{-(\lambda_1 t+\lambda_2^* t)} + \alpha_2\alpha_1^* e^{-(\lambda_2 t+\lambda_1^* t)}$ can be ignored here. This can also be applied to the terms, $\rho_{a_2 a_2}(t)$ and $\rho_{bb}(t)$.

Fig. 2 Quantum beats in the population oscillations with a ratio of dipole moments of **a** $\alpha = 0.6$, two upper level spacing of **b** $\omega_{12} = 2.0\gamma_{20}$, **c** spontaneous emission spectra, and **d** two-photon correlations. Other parameters are the same as those in Fig. 1
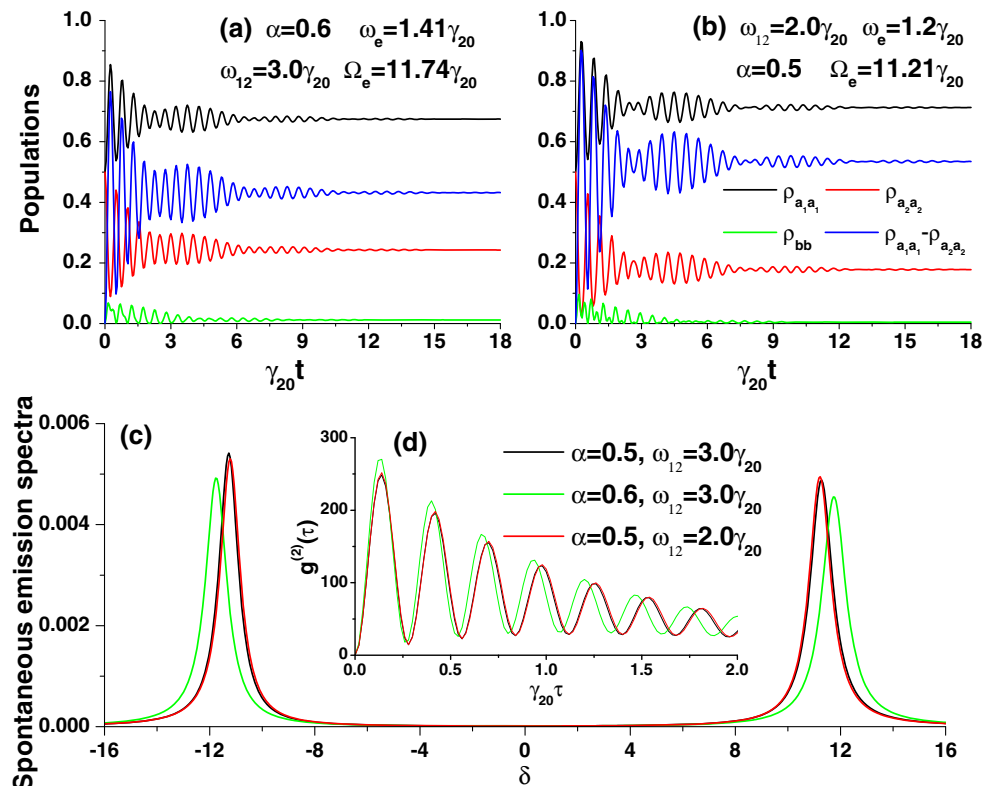
After the simplification, the second term of $\rho_{a_1a_1}(t)$ becomes:

$$\rho_{a_1a_1}^{(1)}(t) \propto \cos \Omega_e t \cos \frac{\omega_e}{2} t. \tag{6}$$

This is the main result of this paper. Ω_e is the frequency of the population oscillations. Its largest contributions come from the Rabi frequencies $\Omega_{1,2}$. Its beat frequency $\omega_e/2$ is determined by the spacing ω_{12} of the two upper levels and the ratio α between the two dipole moments. The mechanism of quantum beats is totally different from that of previously reported QI phenomena, which are caused either by external excitation fields [1–5] or by the environment in which the atoms are embedded [6–10]. Physically, this kind of quantum beat originates from the interference between transition channels with different dipole moments, and its frequency is determined by the intrinsic atomic parameters ω_{12} and α. In this case, the parameters $\gamma_{20} = 1.0$, $|\vec{\mu}_2| = 1.0$, and $\Omega_2 = 10.0\gamma_{20}$. When $\omega_{12} = 3.0\gamma_{20}$ and $\alpha = 0.5$, we can clearly observe the oscillations in the populations and their quantum beats with the frequencies $\Omega_e = 11.24\gamma_{20}$ and $\omega_e/2 = 0.9\gamma_{20}$, respectively (Fig. 1). The population

transfer between $|a_1\rangle$ and $|a_2\rangle$ is shown by the beat terms of the population inversion $\rho_{a_1a_1} - \rho_{a_2a_2}$. In addition to $\rho_{a_1a_1}$ and $\rho_{a_2a_2}$, there is also a slight beating in the population oscillations in the lower level ρ_{bb}.

The effects of the upper level spacing ω_{12} and dipole moment ratio α on quantum beats are discussed. From above formulas, we see that for a fixed ω_{12} and increasing α, the effective Rabi frequency Ω_e increases and the beat frequency ω_e decreases. This is numerically shown in Figs. 1 and 2a. By contrast, when α is fixed and ω_{12} is increasing, the beat frequency $\omega_e/2$ also increases, but the Ω_e remains relatively stable. This can be seen in Figs. 1 and 2b.

Generally, quantum beats in atomic populations can not be measured directly. Therefore, we calculated the spontaneous emission spectra $S(\omega_k)$ with $\delta = \omega_k - 0.5(\omega_{a1} + \omega_{a2}) + \omega_c$ and two-photon correlations $g^2(\tau)$ ($|a_1\rangle \leftrightarrow |b\rangle$ and $|a_2\rangle \leftrightarrow |b\rangle$) in the framework of quantum regression theory [1, 2, 20]. As shown in Fig. 2c, d, spontaneous emission cancellation [1, 2] and the Rabi oscillation of the two-photon correlations occur for an effective Rabi frequency Ω_e. If one of the atomic parameters, ω_{12} or α, is known, the other parameter can

Fig. 3 a Schematic of the silver nanoantenna used to excite the atoms and b its normalized absorption. Here, the incident field with $E_0 = 1.0$ propagates along the z-axis and is polarized along the x-axis. c Near-field distributions E_x and E_z and d modified decay rates γ_{xx} and γ_{zz} for the xy-plane of 50 nm from the metallic surface
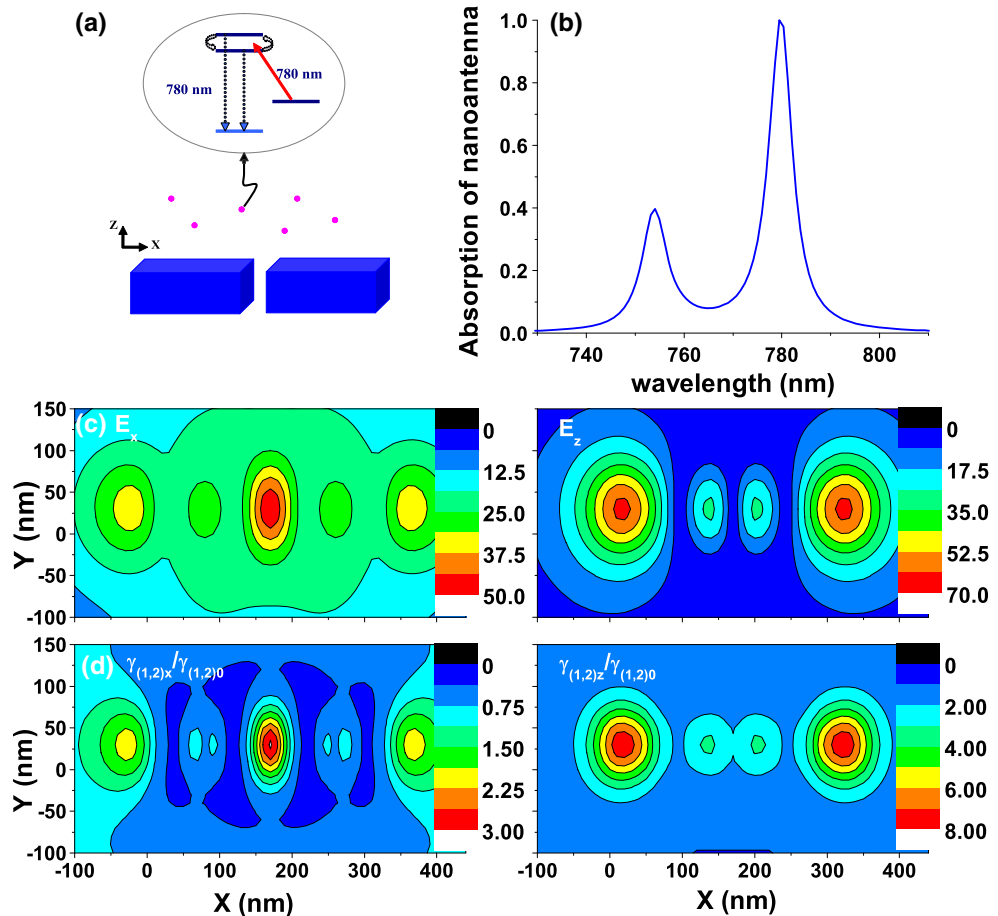
be monitored via the changes in the Rabi frequencies. Therefore, the system may have potential applications in the measurement of dipole moments [18].

## Nanoscale Realization Through Resonant Plasmonic Antenna

This quantum beat phenomenon can also be demonstrated in the anisotropic vacuum, induced by the anisotropy of the local states density of collective oscillations of the free electrons in the plasmonic structure [10, 14, 15]. The resonant optical nanoantenna [19], as a representative of surface plasmons, can provide nanoscale excitation of atoms and nanoscale decay rate modifications, though with the present technology it is difficult to locate an atom with nanometer accuracy and stability near the antenna. Here, using the Green's tensor technique [24, 25], we designed a nanoantenna composed of two $150 \times 50 \times 50$-nm^3 silver nanostripes with a 30-nm gap (Fig. 3). Its dipole resonance is at the wavelength of 780 nm and quadrupole resonance is at 754 nm. Then we placed the atoms with dipole transitions at 780 nm in the near-field region of the nanoantenna. Only at a distance of 30∼100 nm from the metallic surface is there a large near-field enhancement and a strong anisotropy of the vacuum. If the atoms are very close to the metal, their huge decay rates will quench all fluorescence [26]. However, for atoms, which are far away from the metal, the anisotropy of the vacuum is too small.

For example, Fig. 3c, d displays the near electric field distributions and decay rate modifications of the *xy*-plane 50 nm from the metallic surface, respectively. In this case, the large near-field enhancement and decay rate modification can ensure the occurrence of a nanoscale excitation and anisotropic vacuum. In some nanoregions, the decay rates can be much less and larger than that in the isotropic vacuum and can result in enhanced and suppressed effects on spontaneous emission, which is typical of cavity QED [27]. We chose a location at the middle point on top of the first nanostripe 50 nm from the metallic surface, where electric fields $E_x = 27.34$, $E_z = 17.59$, and $\gamma_{(1,2)x}/\gamma_{(1,2)0} = 0.6807$ and $\gamma_{(1,2)z}/\gamma_{(1,2)0} = 2.374$. Here, $\omega_{12} = 3.0\gamma_{20}$ and $\alpha = 0.5$. To ensure the significant beats, the Rabi frequencies were normalized by 1/3 of amplitude of the electric fields. With varying θ, the beat frequency $\omega_e/2$ does not change, but the effective Rabi frequency Ω_e changes dramatically. As shown in Fig. 4, the amplitudes of the quantum beats of the trapped populations and Rabi frequency in fluorescence spectra and two-photon correlations are very sensitive to θ. Thus, the anisotropy of vacuum and local field enhancement near the resonant plasmonic antenna allow for the nanoscale realization of this quantum phenomenon.

To test this phenomenon experimentally, we propose a scheme to use the rubidium 85 D2 transition hyperfine structure. This four-level system is

Fig. 4 Quantum beats in population oscillations with various spatial angles for **a** $\theta = 0.0\pi$, **b** $\theta = 0.25\pi$, and **c** $\theta = 0.5\pi$ and **d** spontaneous emission spectra and **e** two-photon correlations. θ is defined in the inset of Fig. 1
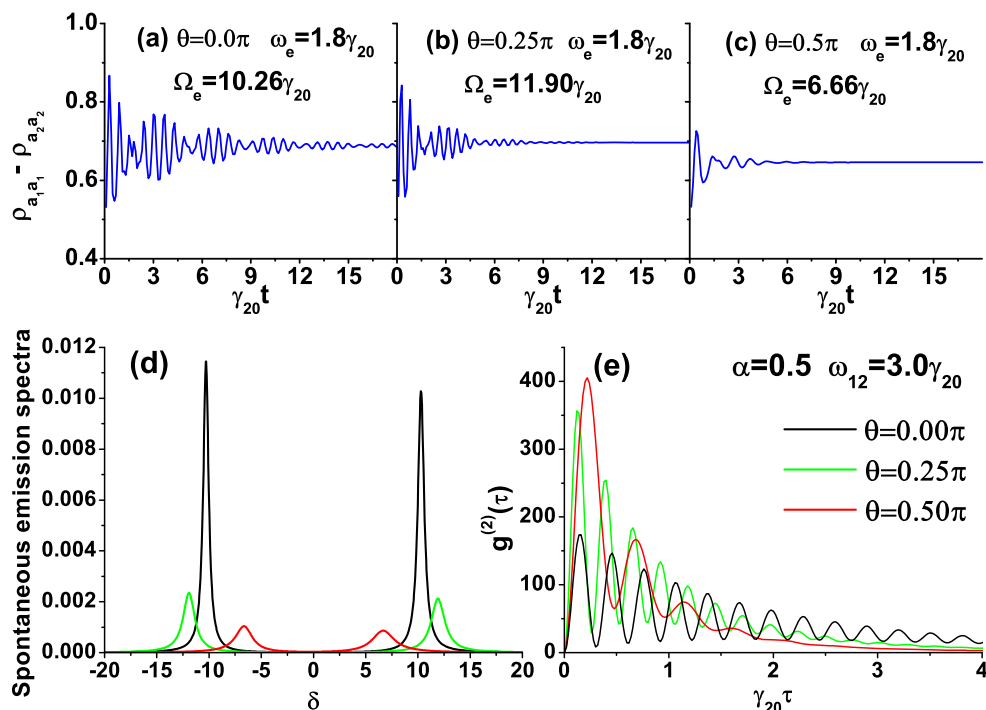
formed by two excited states $|a_1\rangle(5^2P_{3/2}, F = 3)$ and $|a_2\rangle(5^2P_{3/2}, F = 2)$ and two ground states $|b\rangle(5^2S_{1/2}, F = 3)$ and $|c\rangle(5^2S_{1/2}, F = 2)$. The hyperfine splitting between two excite states is $\omega_{12} = 63\,MHz$, and the decay rate of the upper state to ground states is $\Gamma = 2\pi \times 6$ MHz (or $\gamma_{20} = 6$ MHz). The dipole moment ratio, α, between $|a_1\rangle \leftrightarrow |c\rangle$ and $|a_2\rangle \leftrightarrow |c\rangle$ is $(14/45)/(7/18) = 0.8$ and $\omega_e = 2.2\gamma_{20}$. If we use a driving electric field with the value of $E = (10.0 - 20.0)\gamma_{20}$, the effective Rabi frequencies are $\Omega_e = (9.0 - 16.0)\gamma_{20}$. Using current nanofabrication techniques, the designed plasmonic structure can be fabricated in the lab. Thus, an experimental test should be possible.

Summary

We have observed intrinsic quantum beats of atomic populations in a coherently driven four-level system. The mechanism of this beat phenomenon is the interference between the transition channels with different dipole moments, and beat frequency is determined by the atomic parameters. Through the changes in Rabi frequency, these parameters can be monitored via spontaneous emission spectra and two-photon correlations. Therefore, the system may be applied in the measurement of dipole moments. We also used a resonant plasmonic nanoantenna to realize the nanoscale control of the amplitude of the quantum beats, the spontaneous emission cancellation, and the Rabi oscillation of the two-photon correlations through the anisotropy of the near field and decay rates.

References

1. Zhu S, Scully MO (1996) Spectral line elimination and spontaneous emission cancellation via quantum interference. Phys Rev Lett 76:388–341
2. Lee H, Polynkin P, Scully MO, Zhu SY (1997) Quenching of spontaneous emission via quantum interference. Phys Rev A 55:4454–4465
3. Paspalakis E, Knight PL (1998) Phase control of spontaneous emission. Phys Rev Lett 81:293–296
4. Paspalakis E, Kylstra NJ, Knight PL (1999) Transparency induced via decay interference. Phys Rev Lett 82:2079–2082
5. Zhou P, Swain S (1999) Phase-dependent spectra in a driven two-level atom. Phys Rev Lett 82:2500–2503
6. Agarwal GS (2000) Anisotropic vacuum-induced interference in decay channels. Phys Rev Lett 84:5500–5503
7. Zhu SY, Chen H, Huang H (1997) Quantum interference effects in spontaneous emission from an atom embedded in a photonic band gap structure. Phys Rev Lett 79:205–208
8. Quang T, Woldeyohannes M, John S, Agarwal GS (1997) Coherent control of spontaneous emission near a photonic band edge: a single-atom optical memory device. Phys Rev Lett 79:5238–5241
9. Yang Y, Xu J, Chen H, Zhu SY (2008) Quantum interference enhancement with left-handed materials. Phys Rev Lett 100:043601
10. Yannopapas V, Paspalakis E, Vitanov NV (2009) Plasmon-induced enhancement of quantum interference near metallic nanostructures. Phys Rev Lett 103:063602
11. Brongersma ML, Shalaev VM (2010) Applied physics. The case for plasmonics. Science 328:440–441
12. Chang DE, Sorensen AS, Hemmer PR, Lukin MD (2006) Quantum optics with surface plasmons. Phys Rev Lett 97:053002
13. Ozel T et al (2008) Selective enhancement of surface-state emission and simultaneous quenching of interband transition in white-luminophor CdS nanocrystals using localized plasmon coupling. New J Phys 10:083035
14. Gu Y, Huang L, Martin OJF, Gong QH (2010) Resonance fluorescence of single molecules assisted by a plasmonic structure. Phys Rev B 81:193103
15. Marty R, Arbouet A, Paillard V, Girard C, ColasdesFrancs G (2010) Photon antibunching in the optical near field. Phys Rev B 82:081403(R)
16. Hendrickson SM, Lai MM, Pittman TB, Franson JD (2010) Observation of two-photon absorption at low power levels using tapered optical fibers in rubidium vapor. Phys Rev Lett 105:173602
17. Lakowicz JR (2006) Plasmonics in biology and plasmon-controlled fluorescence. Plasmonics 1:5–33
18. Lange W, Mlynek J (1978) Quantum beats in transmission by time-resolved polarization spectroscopy. Phys Rev Lett 40:1373–1376
19. Mühlschlegel P et al (2005) Resonant optical antennas. Science 308:1607–1609
20. Scully MO, Zubairy MS (1997) Quantum optics. Cambridge University Press, Cambridge
21. Novotny L, Hecht B (2006) Principles of nano-optics. Cambridge University Press, Cambridge
22. Barnett SM et al (1996) Decay of excited atoms in absorbing dielectrics. J Phys B 29:3763–3781
23. Li G, Li F, Zhu SY (2001) Quantum interference between decay channels of a three-level atom in a multilayer dielectric medium. Phys Rev A 64:013819
24. Gu Y et al (2008) Resonance capacity of surface plasmon on subwavelength metallic structures. EPL 83:27004
25. Martin OJF, Girard C, Dereux A (1995) Generalized field propagator for electromagnetic scattering and light confinement. Phys Rev Lett 74:526–529
26. Dulkeith E et al (2002) Fluorescence quenching of dye molecules near gold nanoparticles: radiative and nonradiative effects. Phys Rev Lett 89:203002
27. Ye J, Vernooy DM, Kimble HJ (1999) Trapping of single atoms in cavity QED. Phys Rev Lett 83:4987–4990